Pastor, JV.; García Martínez, A.; Mico Reche, C.; Garcia-Carrero, AA. (2020). Experimental Study of the Influence of Gasoline-Diesel Blends on the Combustion Process and Soot Formation under Diesel Engine-Like Conditions. Energy & Fuels. 34(5):5589-5598. https://doi.org/10.1021/acs.energyfuels.0c00091

Experimental study of the influence of Gasoline-Diesel blends on combustion process and soot formation under diesel engine like conditions.

José V. Pastor, A. García, Carlos Micó, Alba A. García-Carrero

CMT - Motores Térmicos /Universitat Politècnica de València

KEYWORDS

Gasoline-Diesel blends

Ignition Delay

Heat Release

Lift-Off Length

Soot

ABSTRACT

Recent research has demonstrated that the reduction in pollutant emissions of diesel engines can be achieved by using high octane fuels such as gasoline, methane or liquefied petroleum gas. Therefore in this study, the focus was to investigate the influence of blends of Diesel and Gasoline on combustion characteristics such as ignition delay, rate of heat release and lift-off length, as well as the influence on soot formation. The experiments were carried out in a test rig with optical access which mimics a single cylinder diesel engine. Four blends were tested: one blend with 100% diesel and then three diesel-gasoline-blends 30%, 50% and70% of gasoline. The blends were made in volumetric proportion and were injected using a common rail injection system without any kind of modification.

The ignition delay and the apparent heat release were studied by means of a pressure transducer. Furthermore, the flame lift-off length and the soot formation were studied using three optical techniques: OH* Chemiluminescence, Natural Luminosity and Diffused Back Illumination extinction imaging (DBI). Different engine operating conditions were analyzed.

Experimental results showed that the ID increased with the increase of gasoline in the blend. Similarly, as the reacting time increased, the lift-off length was longer. On the other hand, the apparent rate of heat release decreased due to the decrease of the mass flow rate, which is dependent on the density of the blend. In addition, differences in the flame radiation were also observed. Gasoline-diesel blends had less luminosity, which is related to less soot formation. To confirm this, the KL factor obtained from the DBI technique was determined and it was concluded that an increase in the proportion gasoline in the blend reduces the soot formation.

INTRODUCTION

The reduction of diesel pollutant emissions, mainly NOx and particulate matter, without penalizing engine consumption is a great challenge for the automotive industry. In order to achieve this objective, the study of new combustion strategies have demonstrated to be a good way to reduce the pollutant emissions and as consequence minimizing the use of after-treatment systems.

One of the most promising strategy is the Low Temperature Combustion (LTC) concept, based on the combustion of premixed and lean fuel-air mixtures[1]. The LTC concept comprises various strategies such as Homogeneous Charge Compression Ignition (HCCI), Partially premixed Compression Ignition (PPCI), Gasoline Compression Ignition (GCI) or Reactivity Controlled Compression Ignition (RCCI)[1].

RCCI strategy is based on using in-cylinder blending of two fuels with different auto-ignition characteristics to control the overall air-fuel mixture reactivity and combustion phasing [2,3]. A Low Reactivity Fuel (LRF) such as Gasoline and a High Reactivity Fuel (HRF) such as Diesel are usually used[3]. While the LRF is injected at the intake manifold, the HRF is injected in the combustion chamber during early stages of the compression stroke in order to control the

overall ignition[4]. In this way, RCCI can reduce NOx and soot emissions while improving thermal efficiency over a wider range of an engine operating range in comparison to other LTC strategies without exceeding mechanical limitations[5,6].

Studies have been made optimizing the RCCI through dual mode[6] to cover the whole engine map. While gasoline injection is always fixed at 10 CAD after the valve opening, for lower loads, diesel is directly injected on the combustion chamber early during compression stroke for extending the mixing time. However, for higher loads, diesel is injected near or even after Top Dead Center (TDC) in order to delay the combustion event [7,8]. Although all these variation of RCCI strategy have shown high potential in terms of efficiency and pollutants emission reduction, the complexity to implement this strategy is to accommodate two different fuel injection systems in the engine hardware [9].Therefore, the necessity of addressing alternatives based on external mixture formation emerges, while keeping the LTC concept based on the dual-fuel combustion.

The dual fuel combustion mode has a challenge, that is to stablish the accurate combustion phase to obtain the maximum performance of LTC strategies[10]. The Combustion phasing depends mostly on the mixture reactivity. It means that it can be controlled with the percentage of LRF added to the blend HRF-LRF to improve the autoignition process[11]. Hence, the start of combustion and later the combustion development for diesel-gasoline blend need to be understood and detailed deeply from a more basic study. Therefore to contribute to this understanding, and moreover provide a solution to avoid the use of two injection system, a detailed fundamental study of spray development of different blends of the most common fuels used in LTC strategies: diesel and gasoline, has been performed in this work, using a single injection system, with the aim of characterizing the autoignition, mixing and combustion process taking place inside the cylinder.

In this work, the combustion behavior of dual fuel and soot formation of four different blends with commercial diesel and gasoline have been studied in a test rig with optical accesses under different diesel-like conditions. Parameters as ignition delay and rate of heat release have been measured through in-cylinder pressure analysis. Furthermore , using optical techniques such as OH* Chemiluminiscense, Broadband Natural flame luminosity (NL) and Diffused Back Illumination Extinction Imaging (DBI), fundamental parameters such as Flame Lift off length and KL (indicator of soot formation) were studied. In addition, the limits of using gasoline-

diesel mixtures have been addressed in terms of combustion effectiveness. This fundamental data will improve the understanding of dual fuel combustion mode through CFD use.

The following sections describe firstly the fuels and blends used. Then, the facility and test matrix are presented, followed by a description of the experimental techniques. Finally, results are discussed, focusing first on combustion performance and later on soot formation.

EXPERIMENTAL METHODOLOGY

1.1 Fuel characteristics

Four different blends of commercial diesel and gasoline have been used for this study. Diesel is considered as the reference fuel due to high reactivity in this study and represents the zero-substitution rate. The other three blends contain 30%, 50% and 70% of gasoline in volume. Additives or lubricity improvers were not added to the blends. Throughout this paper, the four blends are identified as “B0” for 100% of Diesel, and “3070”, “5050” and “7030” for the blends with 30%, 50% and 70% of gasoline respectively. The main properties for the two components are detailed in Table 1.

Parameter	Gasoline	Diesel
Density at 15ºC[kg/m^3]	755	834
Viscosity [mm^2/sec]	at 18ºC[0.65]	at 40ºC [2.7]
Lower heating value [MJ/kg]	41.2	43.0
Auto ignition [ºC]	400°C	[254-285]
Research cetane number	--	53
Research Octane Number	103	--

Table 1. Fuel Properties.

1.2 Experimental facility

Experiments were carried out in a test rig with optical access with three-liter displacement, a 15.6:1 compression ratio and a low rotational speed of 500 rpm, which is described in detail in [12]. The facility enables high-temperature and high-density conditions to be reached in a

cylindrical shaped combustion chamber. It has one upper port for the fuel injector and four lateral, orthogonal accesses. One is used for the pressure transducer while the other three are equipped with quartz optical windows with geometrical dimensions of 88 × 37 mm and 28 mm thickness. The cross-sectional view of the cylinder head is shown in Figure 1.

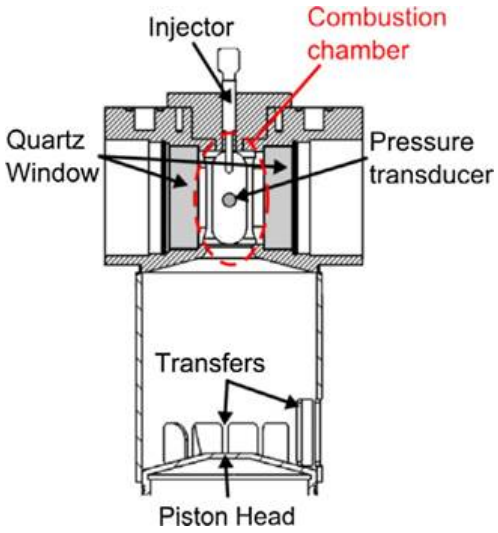

Figure 1. The cross-sectional view of cylinder head. [13]

Intake and exhaust processes are handled by transfers on the liner. The control of the engine conditions is done with intake air pressure and air temperature. The first one is regulated by an external compressor while a set of electrical resistors at the intake line is used to achieve the desired temperature. An injection takes place every 30 cycles, which guarantees that there is no remaining residual gas from previous combustion cycles and that the in-cylinder ambient conditions are kept constant between consecutive repetitions. During engine operation, the block temperature is controlled by an external heating-cooling system.

The facility can be operated in either open or closed loop. The second mode allows modifying oxygen concentration to simulate EGR conditions. Due to the low amount of fuel injected per cycle, N_2 needs to be used to partially replace oxygen in the air. During each test, the O_2 concentration is monitored to ensure that it is kept close to the desired value.

An electronically controlled Bosch common-rail capable to achieve injection pressures up to 160 MPa and equipped with a piezoelectric injector of single-hole nozzle, was used in these experiments. The outlet diameter is 140 μm with a conical shape (K factor of 1.5), which has also been used in different studies by the authors [13–16]. The injection frequency is low during operation and the injector holder is cooled, which allows the nozzle tip and injected fuel temperature to be constant. The injection was placed 3 CAD after TDC and the energizing time was 3 msec.

1.3 Operating conditions

Four ambient conditions have been considered for this study, which are summarized in Table 2. An ambient density of 22.8 kg/m^3 at Top Dead Centre (TDC) was kept constant, while the temperature at TDC was varied, between Low Temperature (780 K), Medium Temperature (830 K) and High Temperature (870 K).

The oxygen concentration was modified to 15% at high temperature conditions to simulate Exhaust Gas Recirculation (EGR). This 15% O_2 concentration corresponds to an engine EGR rate between 28% and 70% for equivalence ratio values between 1 and 0.4 respectively. In all cases, three rail pressures of 500 bar, 1000 bar and 1500 bar were considered. Each fuel was tested under these operating conditions.

For all experiments performed within the present study, 30 injections have been recorded to reduce the measurement uncertainties due to engine operating variability.

The in-cylinder conditions required by the test plan were calculated using the methodology previously described by Pastor[17,18]. In that procedure. The thermodynamic conditions are calculated from the cylinder pressure using a first-law thermodynamic analysis considering blow-by, heat transfer and mechanical stress. Because of compression, air temperature and

density vary with crankangle along the engine cycle and, consequently, during the injection event conditions are not constant. However, in this study it was assumed that temperature of the air interacting with the spray was constant and homogeneous, and the values of temperature and density are averaged during a given time interval. For the purpose of this study, the average interval was considered that between the start of injection and ignition. During such interval, temperature variation was always lower than 1%."

Operating Condition	Injection Pressure [bar]	Temperature [K]	Density [kg/m^3]	Oxygen [%]]
LT	500/1000/1500	780	22.8	21
MT		830	22.8	21
HT		870	22.8	21
LO2		870	22.8	15

Table 2. Test Matrix

1.4 Experimental techniques

1.4.1 Pressure signal analysis

The in-cylinder pressure registered during the combustion cycles has been used to quantify ignition delay (ID). An AVL GU13P pressure transducer coupled to a Kistler 5011 charge amplifier is used for this purpose. The acquisition is synchronized through the flywheel encoder signal, corresponding to a 6 KHz sampling frequency. The system was configured so the motored cycle prior to the one with combustion was recorded. Thus, a difference between them is calculated (ΔP) and the ID is defined as the time elapsed between the injector's start of energizing (SOE) and the first instant when the pressure rise exceeds twice the standard deviation of time-averaged ΔP.

The pressure signal is also used to obtain an apparent heat release (AHR) and rate of heat release (ARoHR). They were calculated based on the application of the first law of thermodynamics to

combustion and motored cycles. It is assumed that the heat transfer is similar for both cycles. In addition, the total amount of fuel injected is negligible in comparison with the trapped air mass, so it is not affecting its thermodynamic properties.

1.4.2 Optical Set up

For the purpose of analysing the effect of the gasoline substitution rate on spray development and soot formation, three different optical techniques have been applied simultaneously: OH* Chemiluminescence (OH*), Diffused Back Illumination (DBI) and Flame Natural Luminosity (NL). A sketch of the optical arrangement is shown in Figure 2.

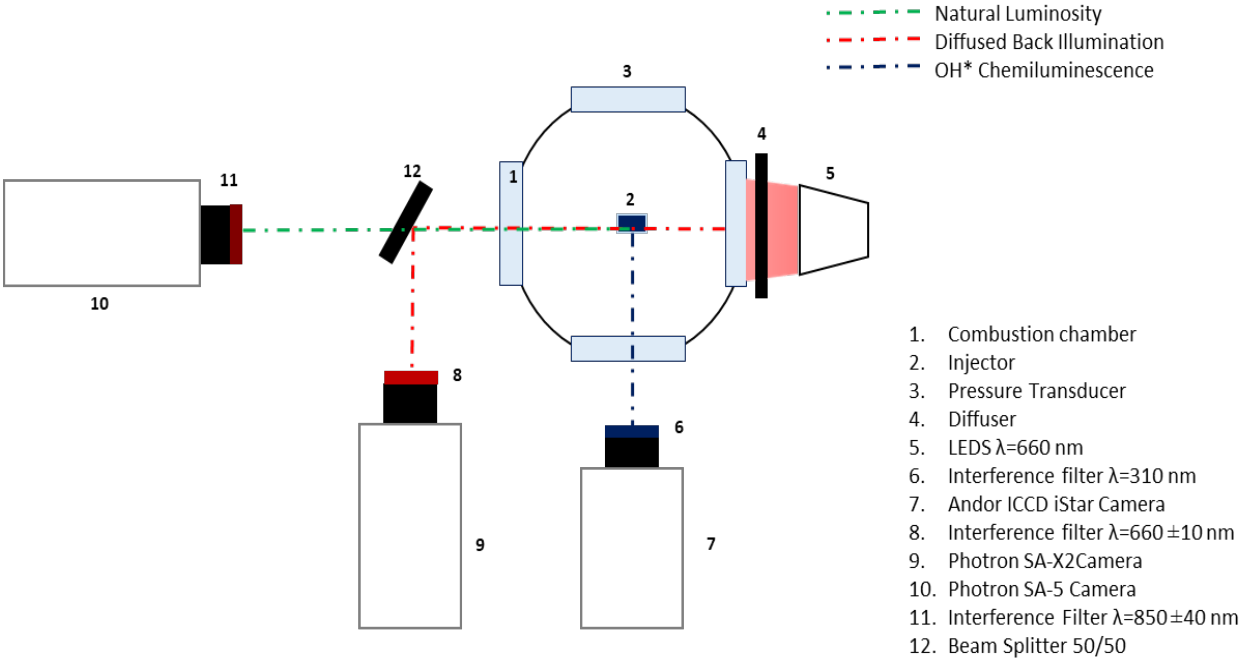

Figure 2. Optical set up

1.4.2.1 OH* chemiluminescence

OH* radicals are accepted as a tracker of high temperature combustion regions in a flame[17,19] such that the visualization of OH∗-chemiluminescence at the base of the flame makes it possible to quantify the Lift-Off Length (LOL).

In this study, the OH* radiation was registered using an Andor Solis iStar ICCD intensified camera equipped with a 100mm focal length f/2 UV objective Bernhard Halle and a 310nm interference filter (FWHM=10nm). A constant intensifier gating of 1 ms was used and only one image per injection event was recorded from 1 ms to 2 ms after start of energizing (ASOE) with an image resolution of 1024x1024 pixeles and a pixel/mm ratio of 9.1. The image processing was done using the approach described in [13], where a background segmentation was applied based on a threshold value, calculated as a percentage of the dynamic range of each image. The LOL was then defined as the average distance between the nozzle and the ten nearest pixels of the flame.

1.4.2.2 Natural Luminosity

Images of Natural Luminosity (NL) are those obtained by registering the broadband radiation of the flame without using any particular optical filter [21]. Taking into consideration the spectral response of the camera, the light collected will almost entirely be in the visible and near infrared range, corresponding to the thermal radiation arising from small soot particles present in the flame. In some cases, it can include a minor contribution of other types of chemiluminescence radiation as well, which can become significant only in low sooting flames. Qualitative and topological descriptions of the soot flame evolution can be obtained, but no quantitative description of the combustion or soot formation is expected. It is well known that flame radiation does not depend only on soot concentration, but also on flame temperature. Nevertheless, flame radiation can be considered as a qualitative indicator of the amount of incandescent soot in the flame [20–22].

In this work, NL images do not contain the whole broadband radiation spectrum. A bandpass filter centred at 850nm (FWHM = 40 nm) was used to avoid registering the light used for the DBI technique. In Figure 2, the optical arrangement used for NL is shown. These images were

recorded with a high-speed camera (Photron Fastcam SA5). The sampling rate was 25 kfps, with a resolution of 336x896 pixels. The exposure time was 40 μsec and a total magnification of 11 pixel/mm. As observed in the figure, a beam splitter with a 50% transmission rate was placed between the camera and the engine to redirect half of the light to the Diffused Back-Illumination extinction imaging (DBI) detector.

1.4.2.3 Diffused Back-Illumination extinction imaging

Diffused Back-Illumination extinction imaging (DBI) technique is based on measuring the amount of light attenuated by the soot particles within the flame, which is related to the soot concentration. Figure 2 shows the optical setup. A red LED (λ = 660nm) was used in these experiments as the light source to create a high-power pulsed illumination. A diffuser was placed in front of the LED to create a diffused Lambertian intensity profile[23]. On the collection side, the transmitted light from the LED and the flame radiation went through a beam splitter with a 50% reflection rate. Then, half of the light was collected by a high-speed CMOS camera Photron SA-X2, with 0.29 μs exposure time, 336×896 pixels resolution, 25 kfps sampling frequency and a pixel/mm ratio of 11.

The images obtained were analyzed, taking into account that the total light registered by the camera includes two parts: the transmitted LED light intensity and the flame radiation. Due to the use of a bandpass filter centered at 660 nm (FWHM = 10nm), the crosstalk of flame radiation into the DBI signal is minimized. However, the flashing frequency of the LED was set as half of the camera frame rate to capture a flame image between every two consecutive LED pulses. Thus, flame luminosity was quantified and used to isolate the transmitted LED light from the total registered radiation. The light attenuation can then be related with the optical properties of soot cloud through the Lambert-Beer's law, as described in Equation (1).

$$\frac{I_{on} - I_{off}}{I_0} = e^{-KL} \qquad \textbf{(1)}$$

I_{on} is the sum of the transmitted LED intensity and the flame luminosity recorded by the DBI camera when the LED is on. I_{off} is the intensity of the flame acquired when the LED is off. I_0 is the LED light intensity obtained from images recorded before the start of injection. *K* is the soot dimensional extinction coefficient and *L* is the light beam path length through the soot cloud. The product KL represents the integral value of the soot extinction coefficient along the light path, which is related with the soot concentration [24]. In this work, the latter analysis has been based on this parameter.

To summarize, settings used for each technique are shown in Table 3

Parameter	Optical Technique		
	OH*	**NL**	DBI
Camera	Andor Solis iStar ICCD	Photron Fastcam SA5	Photron SA-X2,
Exposure time (msec)	From 1 to 2	0.04	0.00029
Filter wavelength (nm)	310 ±10	850 ±40	660±10
Resolution (pixel)	1024x1024	336x896	336x896
Frame rate (kfps)	Single frame	25	25
Pixel/mm	9.1	11	11

Table 3. Main characteristics of the optical techniques used

RESULTS AND DISCUSSION

1.5 Effect of fuel composition on Global combustion Parameters

1.5.1 Auto-ignition effectiveness

Previous to the analysis of the effect of the different diesel-gasoline blend ratios over the combustion process, it has been considered important to address the feasibility of introducing

a low reacting fuel, like gasoline, into a compression ignition engine. For this purpose, the effectiveness of auto ignition has been calculated for the four blends, under all operating conditions considered in this study. This parameter has been defined as the percentage of the cycles/repetitions carried out for each blend in which combustion takes place. The diagnostic has been based on the in-cylinder pressure signal, using the same criterion as the one described for ignition delay calculations.

From this analysis, it has been observed that the combustion takes place in 100% of the cases for fuels B0, 3070 and 5050. For 7030, due to the high proportion of gasoline in the mixture and its low reactivity, there are operating conditions in which combustion does not occur. These are low temperature (LT) and at low oxygen concentration (LO_2). For the first case, effectiveness was 73 % at 500 bar of injection pressure and as injection pressure increases, the effectiveness reduces to 13% at 1000 bar and 7 % at 1500 bar respectively. For the second case, no autoignition was observed.

1.5.2 Effect on Ignition Delay

Ignition delay was defined, through in-cylinder pressure, as the time elapsed between start of energizing (SOE) and the first instant when there is a pressure rise, when the start of combustion is detected. Results shown in Figure 3 correspond to the average of 30 cycles tested.

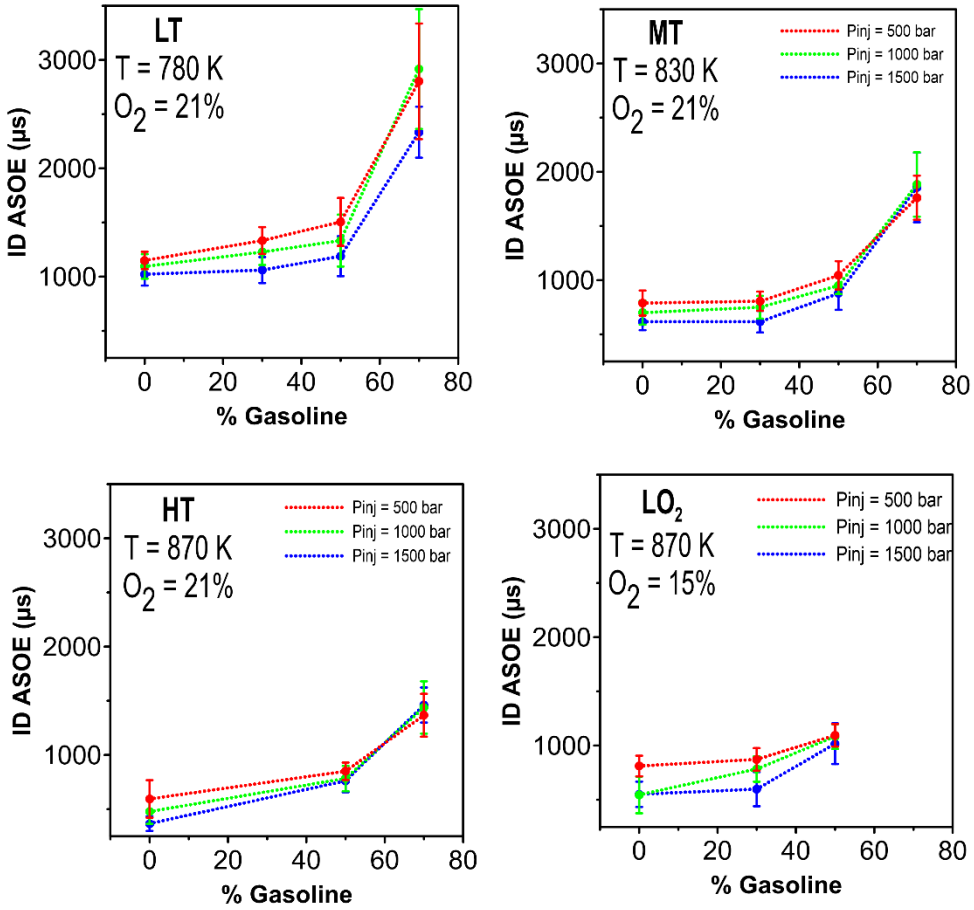

Figure 3. Ignition delay related to gasoline blend ratio, for each operating condition

The ignition delay can be observed in Figure 3 for each blend, which is represented in the abscissa axis as the volume fraction of gasoline in the blend (in percent). In addition, the influence of operating conditions on the ignition delay is presented for the three injection pressures. It is worth mentioning that for LO2, the ID values corresponding to 7030 have not been represented because there was not combustion in any cycle. For the LT case, effectiveness was very low and consequently standard deviation of ID in Figure 3 is higher than for the other cases.

Figure 3 also shows a clear correlation between the ignition delay and the reactivity of the fuel. Therefore, the ID for B0 is the lowest due to the high reactivity of the diesel and, in the opposite case, 7030, it is the highest. As a reference, for MT at 1000 bar of injection pressure, the increase

in the ID between B0 and the blends is 50 µs, 250 µs and 1183 µs for 3070, 5050 and 7030. This represent an increment of 7% 35% and 270% respectively. Thus, the increase is not linear with the gasoline content. Furthermore, it is observed that the difference between 5050 and 7030 is bigger than difference between 3070 and 5050. It is expected that the cetane number would be reduced as the proportion of gasoline in the blend increases [25,26], which agrees with the behavior observed in this study. Additionally, Han [27] reports that cetane number is the most dominant factor on the ignition delay time. Another important observation is the change in the gradient between 5050 and 7030 for MT and HT conditions. The gradient is less steep for the HT operating condition. The difference between these two blends for MT conditions is around 933 µs (98%) whereas for HT it is 656 µs (83%), as the higher temperatures promote faster reaction rates.

The effect of temperature and injection pressure on ignition delay is in line with previous studies[28,29], which indicate that an increase of both parameters reduce the ID. On the other hand, a decrease in the oxygen concentration increases the ID due to the fact that the air-fuel blend is less reactive. However, in the case of 7030, the variation of injection pressure does not seem to have an effect on the ID, as the values are very close and the differences between each one is very small. The chemical characteristics of the blend cause a higher delay that avoid observing the effect of injection pressure.

1.5.3 Effect on Heat Release

Based on the in-cylinder pressure signal, the apparent rate of heat release (ARoHR) and apparent heat release (AHR) were calculated for the four blends and for the different operating conditions. Figure 4 presents the evolution of both magnitudes during the combustion cycle for the blends and the operating conditions considered in this work.

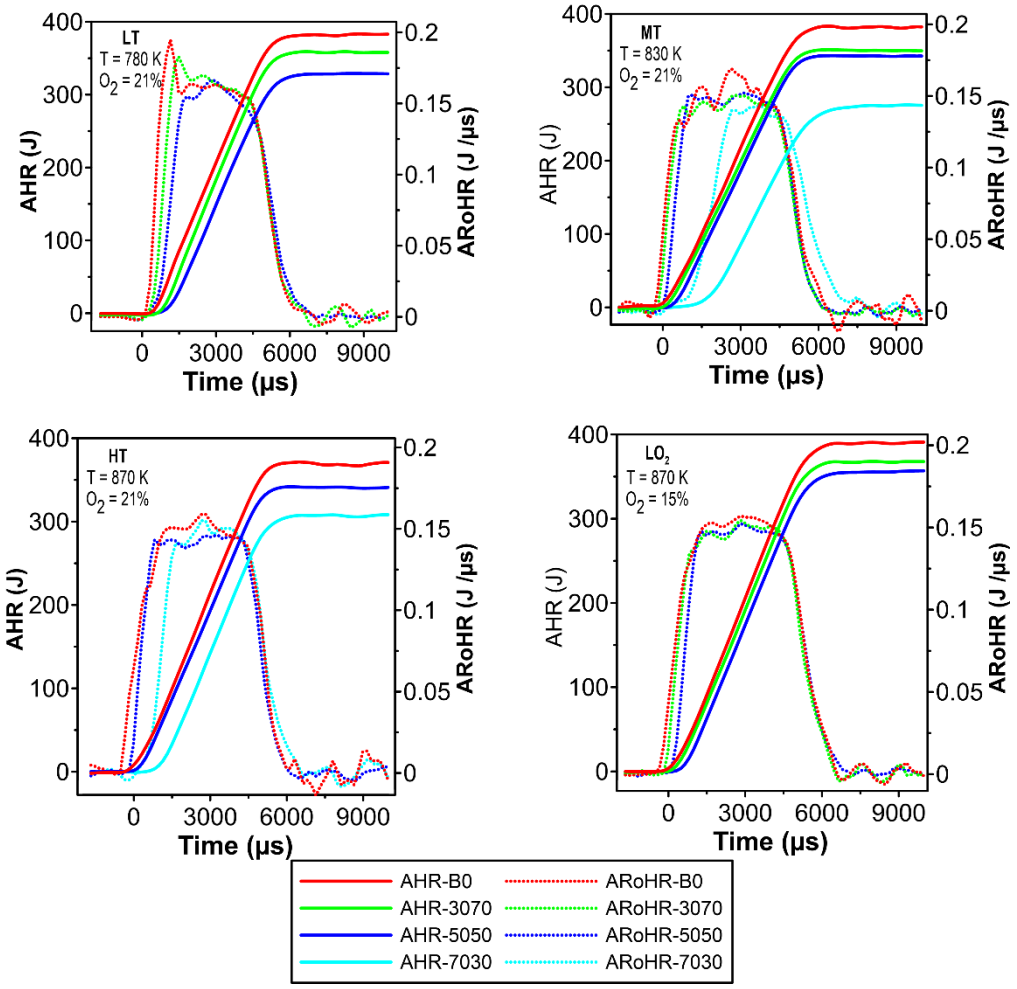

Figure 4. Apparent heat release (AHR) and apparent rate of heat release (ARoHR) for each blend at different operating conditions and 1000 bar of injection pressure

In general, it is possible to see that an increase in the gasoline fraction in the blend reduces the heat released. Due to its lower reactivity, the ID increases and thus the energy from the fuel starts to be released later in the cycle. However, it can also be observed that combustion finishes more or less at the same time. As a consequence, the AHR is lower. Furthermore, differences also arise when comparing the stabilized part of the ARoHR curves. As it was stated by Pastor [14], the mass flow rate of gasoline-diesel blend varied with the blend ratio. The more gasoline, the less fuel injected. The authors related this behavior mainly to differences in fuel density, based on equation (2):

$$\dot{m}_{blend} = C_v \cdot \sqrt{2 \cdot (P_{inj} - P_{cc}) \cdot \rho_f} \cdot A_{eff} \qquad \textbf{(2)}$$

Where $\dot{m}_{blend}$ corresponds to mass flow rate, ρ_f is the fuel density, C_v is the velocity coefficient, A_{eff} is the effective area of the orifice, P_{inj} is the injection pressure and P_{cc} is the

pressure inside the combustion chamber. Additionally, results presented in [14] were obtained with the same injection system and operating conditions. Thus, they have been used in this paper to confirm the differences observed in ARoHR between blends. Equation (3) shows the relationship between chemical rate of heat release (ARoHR) and the mass flow rate of B0 and each one of the blends. ARoHR corresponds only to the amount of energy available in the fuel, $\dot{m}_{B0}$ and ρ_{B0} refer to the mass flow rate and density of pure diesel and LHV_{blend} is the Low Heat Value for each blend assessed.

$$ARoHR_{blend} = \dot{m}_{B0} \cdot \sqrt{\frac{\rho_{blend}}{\rho_{B0}}} \cdot LHV_{blend} \quad \textbf{(3)}$$

Table 4 shows the comparison between B0 and the other blends. The similarities observed between the experimental results and the calculations confirm the observed trends and justify that the differences of ARoHR between the blends are due to their different densities and lower heating values.

Fuel	$RoHR_{blend}/RoHR_{B0}$ **Calculated (%)**	$RoHR_{blend}/RoHR_{B0}$ **Experimental (%)**
3070	91.34	91.80
5050	87.83	89.98
7030	69.11	71.95

Table 4. Comparison between calculated and experimental rate of heat release with respect to B0 at MT operating conditions and 1000 bar of injection pressure

The lower ARoHR is reflected directly in a reduction of the total heat release. Therefore, the longer ID mentioned previously, together with the difference in rate of heat release, cause a reduction of the AHR when the content in gasoline increases, reaching a difference of up to around 10% between B0 and 3070 and 5050, whereas in the case of 7030, the difference with respect to B0 is approximately 30% at the MT operating condition.

1.5.4 Effect on Lift-off Length

Figure 5 shows the lift-off length (LOL) for each blend at the operating conditions defined in this paper. The abscissa axis represents the volume fraction of gasoline present in the blend as a percentage. Again, for LT and LO_2 operation conditions, LOL values corresponding to 7030 are not represented due to the low combustion effectiveness.

The trends observed for LOL are similar to those reported for ID. When the content of gasoline in the blend increases, the LOL increases too.

Analyzing the effects of boundary conditions, it can be observed that the results correspond to those found in the literature[28–30]. LOL decreases with increasing ambient temperature and density, as it reduces the amount of air required to burn the fuel injected.

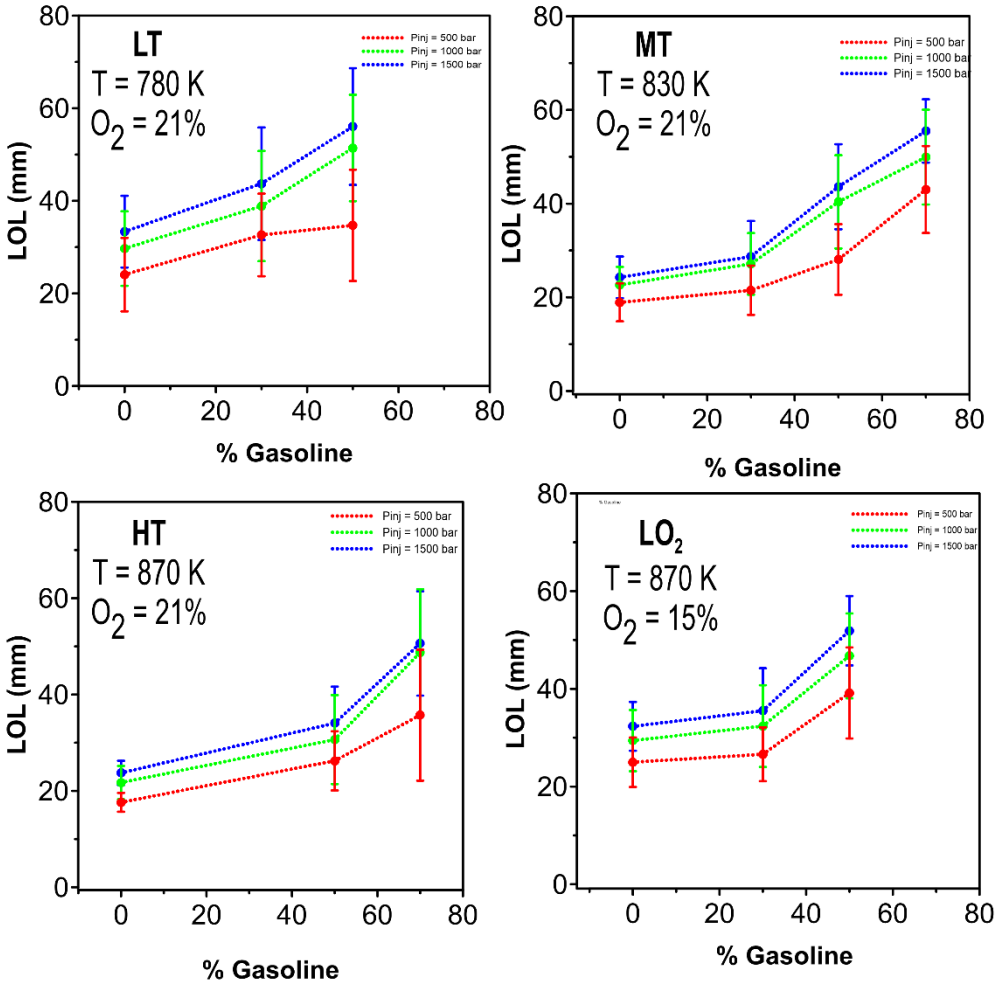

Figure 5. Lift-off Length for each operating condition and each blend

In addition, Figure 5 shows that the standard deviation is higher when the blends contains gasoline and therefore the gasoline addition made it difficult to achieve lift-off stability

1.6 Effect of fuel composition on soot formation

For the study of soot formation, the cases with a higher content of diesel (B0) and gasoline (7030) are represented, as well as an intermediate blend (5050) to verify the observed trend. Therefore, from now on, the analysis will be for B0, 5050 and 7030.

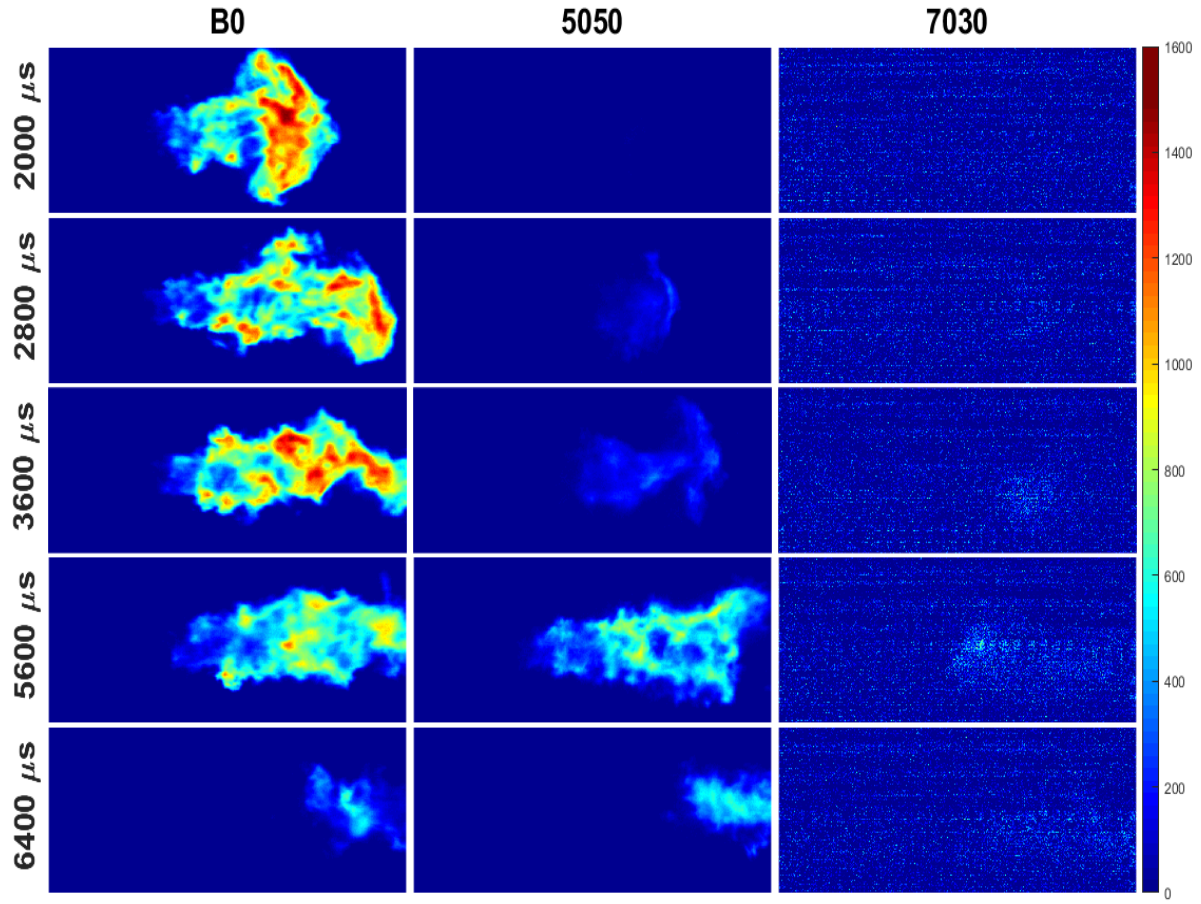

Figure 6. Flame natural luminosity for blends tested at MT operating conditions and 1000 bar of injection pressure. 7030 intensity levels have been increased 30 times

Figure 6 shows the flame natural luminosity for blends tested at MT operating conditions and 1000 bar of injection pressure. A temporal evolution is represented, by means of several frames recorded with the high-speed camera. For 7030, the luminosity did not reach sufficient intensity levels to be compared with others blends. For that reason, it has been increased 30 times and even so, it is not possible to observe the flame intensity of 7030. Images shown in Figure 6 correspond to single combustion cycles.

The amount of natural radiation registered does not just depend on the soot concentration, but also on the temperature[21]. If it is considered that all blends have the same flame temperature, a qualitative analysis of soot formation can be done. Thus, in Figure 6, it can be observed that soot formation decreases with the increase of gasoline in the blend. In addition, soot appears later and also farther from the injector. This is coherent with the results reported previously. Both ID and LOL increase with the gasoline volume fraction, allowing more air entrainment

before combustion and hence a more homogeneous mixture, which leads to a decrease in soot formation.

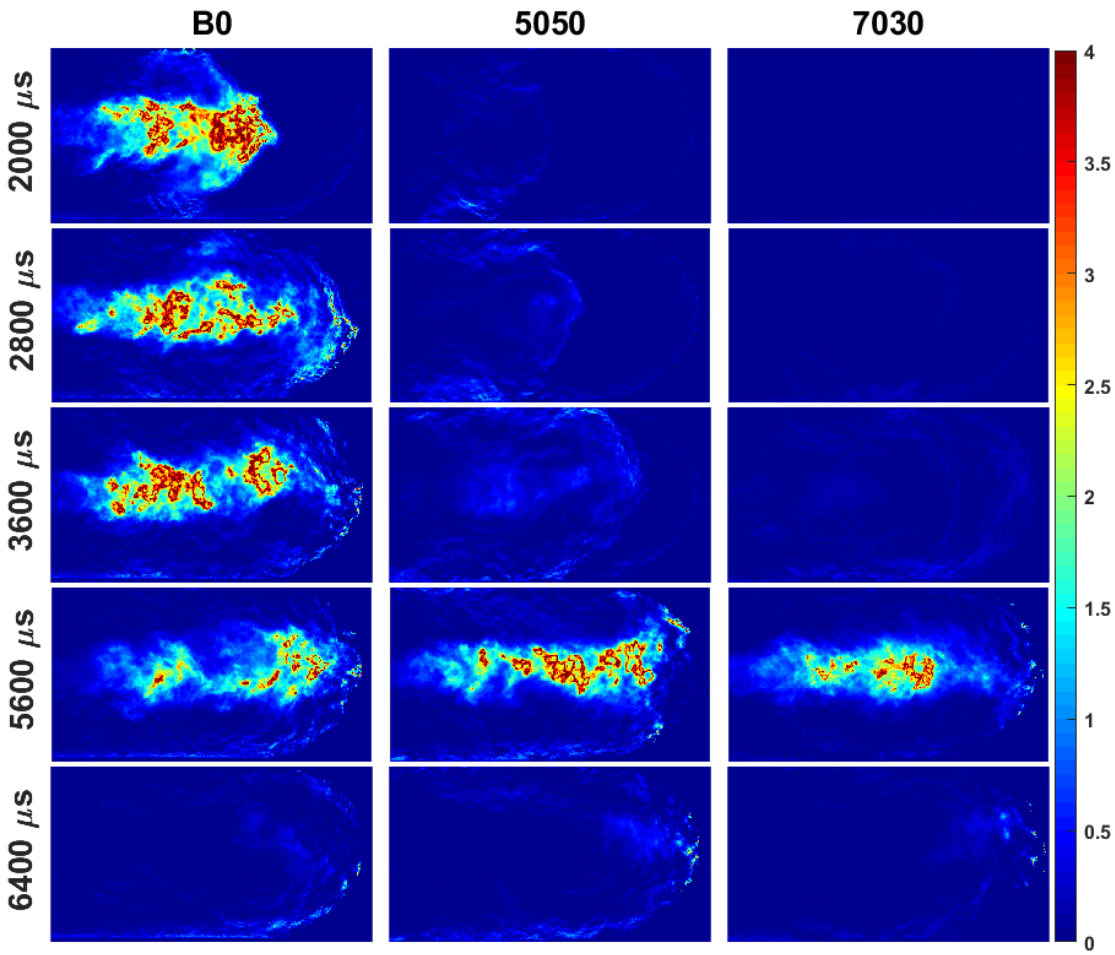

Figure 7. Light extinction for each blend at MT operating condition at 1000 bar of injection pressure. The scale (on right hand side) represent the KL parameter

In order to quantify the soot formed, images from DBI were used to determine the soot KL factor. It is an indicator of the flame soot concentration, as was explained in the methodology section. Figure 7 represents the light extinction obtained for each blend at the MT operating conditions and 1000 bar of injection pressure. These images correspond to a single combustion cycle; the same one that was used in Figure 6 in the same time interval.

In Figure 7, it can be observed that the combustion behavior is similar to that studied with the pressure transducer and also with natural luminosity; when the gasoline content in the blend is greater, the combustion starts later and therefore the soot also appears later. In addition, an increase in the amount of gasoline produces a lower concentration of soot.

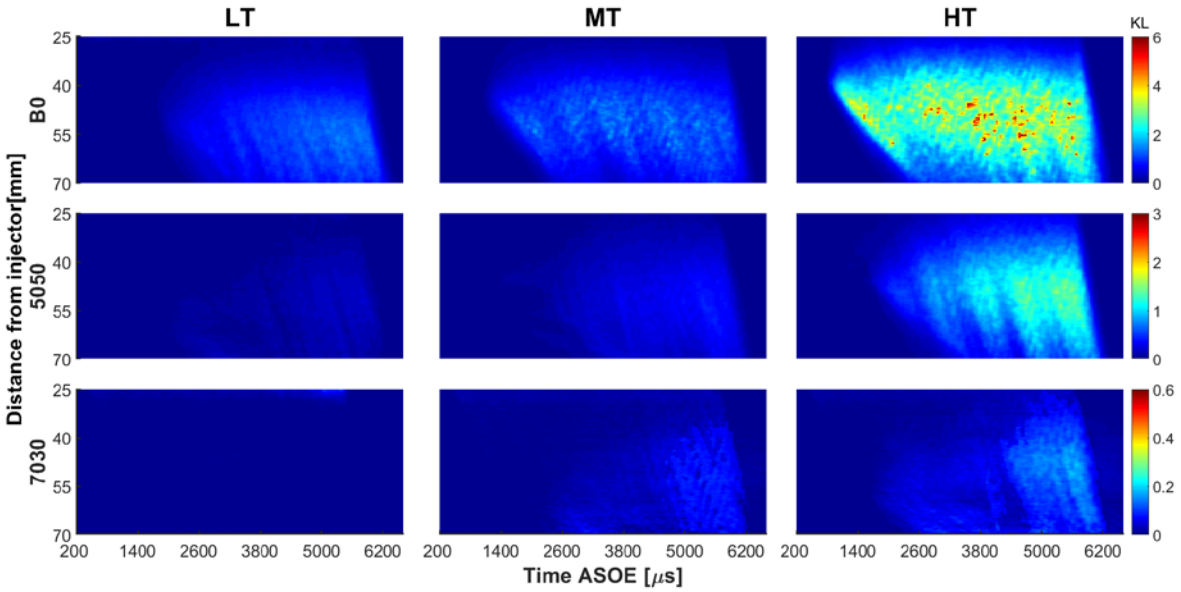

Figure 8. Temporal and Spatial KL evolution at 1000 bar for LT, MT and HT operating conditions

Figure 8 represents the spatial and temporal evolution of soot KL, as an average of the 30 repetitions tested. In Figure 8, the KL value is averaged along the radial direction of the flame. Thus, for each instant recorded, the corresponding KL image is transformed into a 1D-vector. After that, all vectors are concatenated to create a 2D-matrix of KL values, which correspond to each map shown in Figure 8. As a result, the vertical axis represents the distance from the nozzle while the horizontal axis represents time ASOE. For a clear visualization of the map, a color scale has been used as a function of the KL values for each blend. Note that the 5050 and 7030 scales are 50% and 10% of the B0 scale respectively.

It can be observed in the maps that as the proportion of gasoline increases, the soot concentration decreases. This is due to the lower reactivity of gasoline, resulting in a longer ignition delay and a longer flame lift-off length, as was discussed previously. Regarding its evolution, it is possible to see that in general, the more gasoline content in the blend, the later the soot appears. Furthermore, its distribution is also less uniform along the cycle. For B0, as soon as soot is visible, the concentration remains at its maximum value almost up to the end of the combustion process. With respect to 7030, the first soot is detected around 2600 μs ASOE. However, its concentration starts increasing between 5000 μs and 6000 μs ASOE, when its maximum is reached.

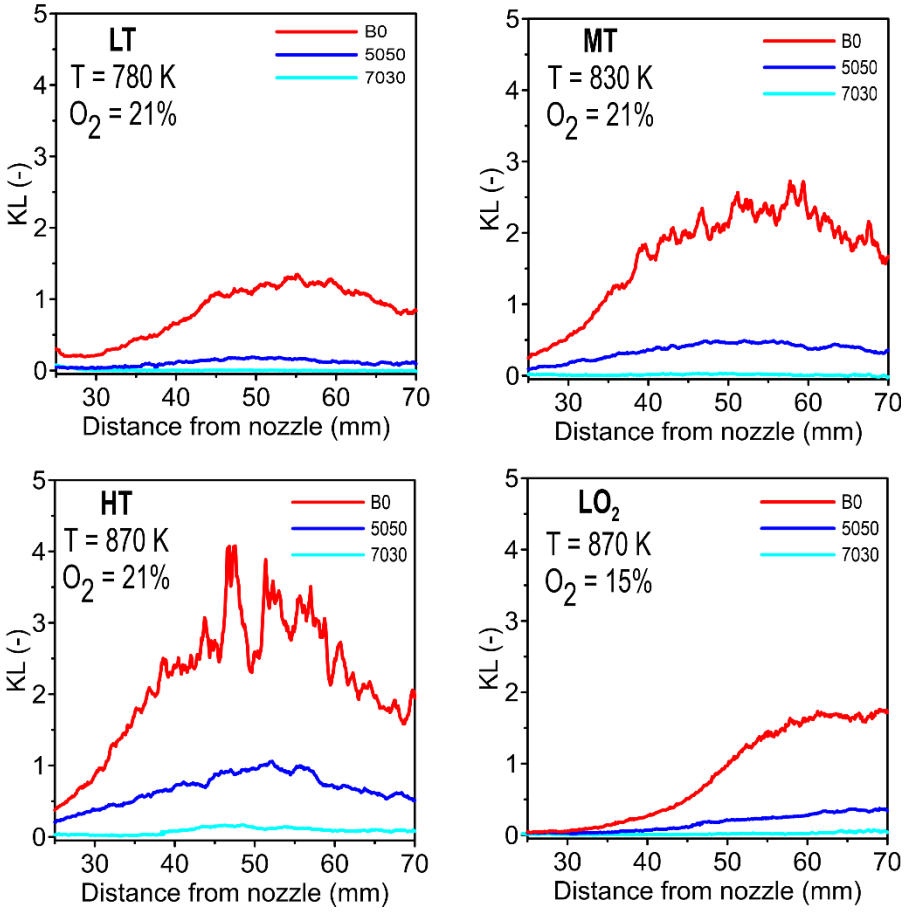

Figure 9. KL evolution through spray axis at 1000 bar of injection pressure and at 5600 μs ASOE

In order to obtain a quantitative comparison, Figure 9 shows the KL evolution along the flame axis at 5600 μs from the start of the energizing. This time has been chosen to ensure that all blends reach a "stabilized" state (eliminating the influences of possible transient phenomena). Results correspond to the average of 30 cycles. The trends discussed previously are also observed in this figure. A higher temperature promotes more soot formation because of a faster combustion process, as the results shown for ID and LOL confirm. Furthermore, a higher percentage of gasoline in the blend ensures the soot reduction for any operating condition. By comparing B0 and 5050 in Figure 9, it is also possible to observe that the difference between the maximum values are slightly larger when the temperature is higher. This could be because at higher temperatures, the diesel autoignition is faster, preventing the formation of a more homogeneous mixture and as consequence, the soot formation is favored.

CONCLUSIONS

Measurements of ID, LOL, heat released, and soot formation were carried out for different gasoline-diesel blends and at different ranges of ambient gas temperature, oxygen concentration and injection pressures.

– It is possible to use gasoline-diesel blends in a compression ignition engine with similar characteristics to those used in this study. It was demonstrated that at least until 50% of gasoline in the blend, the combustion effectiveness is not affected, even in operating conditions with low temperatures and low oxygen concentration, where the reaction velocity is slow. At 70% of gasoline the combustion effectiveness was seriously reduced when the temperature and oxygen concentration were 780 K and 15% respectively

- Gasoline–diesel blends present lower reactivity compared to pure diesel. It decreases when increasing the gasoline ratio. As a consequence, the ignition delay and Lift-Off Length were affected, both increasing with the gasoline volume fraction. When gasoline was increased 30% in the blend, ID increased around 7% and LOL almost 20% at 830 K 1000 bar of injection pressure respect to B0. The tendency was similar for other temperature, oxygen concentration and injection pressure. For 50% of gasoline the increment was 35% for ID and 70% for LOL respect to B0. However, for 70% of gasoline the increment was very high: 2.7 times for ID and 2.15 times respect to B0 for 830K and 1000 bar. Thus, the increment is not linear with the gasoline content.

- A delay in the start of combustion had an impact on heat release. It was observed that it started later in the cycle for the less reactive blends, but finished almost at the same time as the more reactive ones. On the other hand, the blend density affected the injection mass flow rate, which also has an impact on the amount of available energy and therefore the heat release during the whole cycle.

- As the gasoline content of the blended fuel was increased, the soot emission was reduced considerably. It has been related with the lower reactivity of the blends, which leads to more fuel-air mixing before auto ignition and therefore a more homogenous mixture. For 50% of gasoline in the blend, the KL was reduced 80% approximately when the temperature was 830 K and the injection pressure was 1000 bar. For 70% of gasoline the difference between KL values was around 90%. The tendency was similar in the other operating conditions.

ACKNOWLEDGEMENTS

The authors acknowledge that this research work has been partly funded by the Government of Spain and FEDER under TRANCO project (TRA2017-87694-R) and by Universitat Politècnica de València through the Programa de Ayudas de Investigación y Desarrollo (PAID-01-18) and (PAID-06-18) program.

ABBREVIATIONS

AHR: Apparent Heat Release

ARoHR: Apparent Rate of Heat Release

ASOE: After Start of Energizing

DBI: Diffused Back Illumination extinction imaging

CFD: Computational Fluid Dynamics

CAD: Crank angle degree

HT: High Temperature

ICE: Internal Compression Engine

ID: Ignition Delay

LOL: Lift-off Length

LO_2: Low oxygen concentration

LT: Low Temperature

MT: Medium Temperature

NL: Natural Luminosity

Pinj: Injection Pressure

SOE: Start of Energizing

TDC: Top Dead Centre

REFERENCES

(1) Murugesa Pandian, M.; Anand, K. Comparison of Different Low Temperature Combustion Strategies in a Light Duty Air Cooled Diesel Engine. *Appl. Therm. Eng.* **2018**, *142*, 380–390. https://doi.org/10.1016/j.applthermaleng.2018.07.047.

(2) Bessonette, P. W.; Schleyer, C. H.; Duffy, K. P.; Hardy, W. L.; Liechty, M. P. Effects of Fuel Property Changes on Heavy-Duty HCCI Combustion; 2007; pp 2007-01–0191. https://doi.org/10.4271/2007-01-0191.

(3) Kokjohn, S. L.; Hanson, R. M.; Splitter, D. A.; Reitz, R. D. Fuel Reactivity Controlled Compression Ignition (RCCI): A Pathway to Controlled High-Efficiency Clean Combustion. *Int. J. Engine Res.* **2011**, *12* (3), 209–226. https://doi.org/10.1177/1468087411401548.

(4) Kokjohn, S. L.; Hanson, R. M.; Splitter, D. A.; Reitz, R. D. Experiments and Modeling of Dual-Fuel HCCI and PCCI Combustion Using In-Cylinder Fuel Blending. *SAE Int. J. Engines* **2009**, *2* (2), 24–39. https://doi.org/10.4271/2009-01-2647.

(5) Benajes, J.; García, A.; Monsalve-Serrano, J.; Boronat, V. Dual-Fuel Combustion for Future Clean and Efficient Compression Ignition Engines. *Appl. Sci.* **2016**, *7* (1), 36. https://doi.org/10.3390/app7010036.

(6) Benajes, J.; García, A.; Monsalve-Serrano, J.; Boronat, V. Achieving Clean and Efficient Engine Operation up to Full Load by Combining Optimized RCCI and Dual-Fuel Diesel-Gasoline Combustion Strategies. *Energy Convers. Manag.* **2017**, *136*, 142–151. https://doi.org/10.1016/j.enconman.2017.01.010.

(7) Benajes, J.; García, A.; Monsalve-Serrano, J.; Boronat, V. An Investigation on the Particulate Number and Size Distributions over the Whole Engine Map from an Optimized Combustion Strategy Combining RCCI and Dual-Fuel Diesel-Gasoline. *Energy Convers. Manag.* **2017**, *140*, 98–108. https://doi.org/10.1016/j.enconman.2017.02.073.

(8) Benajes, J.; García, A.; Monsalve-Serrano, J.; Boronat, V. Gaseous Emissions and Particle Size Distribution of Dual-Mode Dual-Fuel Diesel-Gasoline Concept from Low to Full Load. *Appl. Therm. Eng.* **2017**, *120*, 138–149. https://doi.org/10.1016/j.applthermaleng.2017.04.005.

(9) Dempsey, A. B.; Curran, S.; Reitz, R. D. Characterization of Reactivity Controlled Compression Ignition (RCCI) Using Premixed Gasoline and Direct-Injected Gasoline with a Cetane Improver on a Multi-Cylinder Engine. *SAE Int. J. Engines* **2015**, *8* (2), 859–877. https://doi.org/10.4271/2015-01-0855.

(10) Singh, A. P.; Agarwal, A. K. Low-Temperature Combustion: An Advanced Technology for Internal Combustion Engines. In *Advances in Internal Combustion Engine Research*; Srivastava, D. K., Agarwal, A. K., Datta, A., Maurya, R. K., Eds.; Energy, Environment, and Sustainability; Springer: Singapore, 2018; pp 9–41. https://doi.org/10.1007/978-981-10-7575-9_2.

(11) Bendu, H.; Murugan, S. Homogeneous Charge Compression Ignition (HCCI) Combustion: Mixture Preparation and Control Strategies in Diesel Engines. *Renew. Sustain. Energy Rev.* **2014**, *38*, 732–746. https://doi.org/10.1016/j.rser.2014.07.019.

(12) Bermúdez, V.; García, J. M.; Juliá, E.; Martínez, S. Engine with Optically Accessible Cylinder Head: A Research Tool for Injection and Combustion Processes. *SAE Tech. Pap.* **2003**. https://doi.org/10.4271/2003-01-1110.

(13) Pastor, J. V.; García-Oliver, J. M.; García, A.; Micó, C.; Möller, S. Application of Optical Diagnostics to the Quantification of Soot in n -Alkane Flames under Diesel

Conditions. *Combust. Flame* **2016**, *164*, 212–223. https://doi.org/10.1016/j.combustflame.2015.11.018.
(14) Pastor, J.; Garcia-Oliver, J. M.; Garcia, A.; Nareddy, V. R. Characterization of Spray Evaporation and Mixing Using Blends of Commercial Gasoline and Diesel Fuels in Engine-Like Conditions. *SAE Tech. Pap.* **2017**. https://doi.org/doi:10.4271/2017-01-0843.
(15) Pastor, J. V.; García-Oliver, J. M.; García, A.; Pinotti, M. Effect of Laser Induced Plasma Ignition Timing and Location on Diesel Spray Combustion. *Energy Convers. Manag.* **2017**, *133*, 41–55. https://doi.org/10.1016/j.enconman.2016.11.054.
(16) Pastor, J. V.; García-Oliver, J. M.; García, A.; Pinotti, M. Laser Induced Plasma Methodology for Ignition Control in Direct Injection Sprays. *Energy Convers. Manag.* **2016**, *120*, 144–156. https://doi.org/10.1016/j.enconman.2016.04.086.
(17) Pastor, J. V.; Payri, R.; Gimeno, J.; Nerva, J. G. Experimental Study on RME Blends: Liquid-Phase Fuel Penetration, Chemiluminescence, and Soot Luminosity in Diesel-Like Conditions. *Energy Fuels* **2009**, *23* (12), 5899–5915. https://doi.org/10.1021/ef9007328.
(18) Pastor, J. V.; García-Oliver, J. M.; Nerva, J.-G.; Giménez, B. Fuel Effect on the Liquid-Phase Penetration of an Evaporating Spray under Transient Diesel-like Conditions. *Fuel* **2011**, *90* (11), 3369–3381. https://doi.org/10.1016/j.fuel.2011.05.006.
(19) Reyes, M.; Tinaut, F. V.; Giménez, B.; Pastor, J. V. Effect of Hydrogen Addition on the OH* and CH* Chemiluminescence Emissions of Premixed Combustion of Methane-Air Mixtures. *Int. J. Hydrog. Energy* **2018**, *43* (42), 19778–19791. https://doi.org/10.1016/j.ijhydene.2018.09.005.
(20) Siebers, D.; Higgins, B. Flame Lift-Off on Direct-Injection Diesel Sprays Under Quiescent Conditions. *SAE Trans.* **2001**, *110*, 400–421. https://doi.org/10.4271/2001-01-0530.
(21) Pastor, J. V.; Garcia-Oliver, J. M.; Garcia, A.; Pinotti, M. Soot Characterization of Diesel/Gasoline Blends Injected through a Single Injection System in CI Engines. *SAE Tech. Pap.* **2017**. https://doi.org/10.4271/2017-24-0048.
(22) Pastor, J. V.; García, J. M.; Pastor, J. M.; Buitrago, J. E. Analysis Methodology of Diesel Combustion by Using Flame Luminosity, Two-Colour Method and Laser-Induced Incandescence. *SAE Tech. Pap.* **2005**, 2005-24–012. https://doi.org/10.4271/2005-24-012.
(23) Xuan, T.; Pastor, J. V.; García-Oliver, J. M.; García, A.; He, Z.; Wang, Q.; Reyes, M. In-Flame Soot Quantification of Diesel Sprays under Sooting/Non-Sooting Critical Conditions in an Optical Engine. *Appl. Therm. Eng.* **2019**, *149*, 1–10. https://doi.org/10.1016/j.applthermaleng.2018.11.112.
(24) Xuan, T.; Desantes, J. M.; Pastor, J. V.; Garcia-Oliver, J. M. Soot Temperature Characterization of Spray a Flames by Combined Extinction and Radiation Methodology. *Combust. Flame* **2019**, *204*, 290–303. https://doi.org/10.1016/j.combustflame.2019.03.023.
(25) Wang, J.; Yang, F.; Ouyang, M. Dieseline Fueled Flexible Fuel Compression Ignition Engine Control Based on In-Cylinder Pressure Sensor. *Appl. Energy* **2015**, *159*, 87–96. https://doi.org/10.1016/j.apenergy.2015.08.101.
(26) Yanowitz, J. *Compendium of Experimental Cetane Numbers*; NREL/TP-5400-67585; National Renewable Energy Laboratory (NREL): Denver West Parkway Golden, CO 80401, 2017; p 78.

(27) Han, M. The Effects of Synthetically Designed Diesel Fuel Properties – Cetane Number, Aromatic Content, Distillation Temperature, on Low-Temperature Diesel Combustion. *Fuel* **2013**, *109*, 512–519. https://doi.org/10.1016/j.fuel.2013.03.039.
(28) Benajes, J.; Payri, R.; Bardi, M.; Martí-Aldaraví, P. Experimental Characterization of Diesel Ignition and Lift-off Length Using a Single-Hole ECN Injector. *Appl. Therm. Eng.* **2013**, *58* (1–2), 554–563. https://doi.org/10.1016/j.applthermaleng.2013.04.044.
(29) Pickett, L. M.; Siebers, D. L.; Idicheria, C. A. Relationship Between Ignition Processes and the Lift-Off Length of Diesel Fuel Jets. *SAE Trans.* **2005**, *114*, 1714–1731. https://doi.org/DOI: 10.4271/2002-01-0890.
(30) Payri, R.; Salvador, F. J.; Manin, J.; Viera, A. Diesel Ignition Delay and Lift-off Length through Different Methodologies Using a Multi-Hole Injector. *Appl. Energy* **2016**, *162*, 541–550. https://doi.org/10.1016/j.apenergy.2015.10.118.